electronics

Review

Performance Enhancement and Stability Improvement in Perovskite Solar Cells via Interface Functionalization

Christos Falaras and Elias Stathatos *

Nanotechnology and Advanced Materials Laboratory, Electrical and Computer Engineering Department, University of the Peloponnese, 26334 Patras, Greece; falarasxristos@gmail.com
* Correspondence: estathatos@uop.gr; Tel.: +30-2610-369242

Abstract: Perovskite solar cells (PSCs) have revolutionized the field of photovoltaics, achieving certified power conversion efficiencies reaching 26% at the laboratory scale. High performance, enhanced stability, and long lifetime are prerequisites for the industrialization and commercialization of this class of third-generation photovoltaic technology. Toward the development of well-performing and robust PSCs against environmental stresses, advanced engineering strategies have been employed, targeting the preparation of perovskite absorbing layers with minimal defects and energy-level fine-tuning hydrophobic contacts. Focusing on both the electron transport layer/perovskite and perovskite/hole transport layer interfaces, this review work encompasses some of the most promising engineering methodologies that were recently proposed in order to optimize the device architecture. Machine learning approaches have also been used to validate experimental data and predict with accuracy solar cell parameters, further confirming the significance and justifying the application potential of the proposed innovative interface functionalization approaches.

Keywords: perovskite solar cells; interface engineering strategies; power conversion efficiency increase; enhanced stability

Citation: Falaras, C.; Stathatos, E. Performance Enhancement and Stability Improvement in Perovskite Solar Cells via Interface Functionalization. *Electronics* **2023**, *12*, 3319. https://doi.org/10.3390/electronics12153319

Academic Editor: Jai Singh

Received: 27 June 2023
Revised: 29 July 2023
Accepted: 31 July 2023
Published: 3 August 2023

1. Introduction

In recent years, intensive research activity has been conducted in the field of third-generation photovoltaics, especially in the development of metal halide perovskite materials and perovskite-based PV devices, where the certified power conversion efficiency (PCE) now reaches 26% [1–5].

Perovskites employed in solar cells are usually described by the general formula ABX_3, where A stands for organic (MA or FA) and/or inorganic (Cs or Ru) cations, B stands for metal cations (Pb or Sn), and X refers to halide anions (I, Br, or X) [6]. A PSC device, independently of its normal or inversed architecture, has a multilayered structure (Figure 1), where the perovskite active layer, which absorbs light and creates photogenerated charge carriers (electrons and holes), is placed between two charge extraction/transport layers (electron transport layer (ETL) and hole transport material (HTM)). A conducting glass substrate (FTO or ITO) below the ETL (HTM) and a metal evaporated film (Au, Ag, or Al) on top of the HTM (or ETL) ensure the charge collection [7]. Despite PCEs outperforming those of silicon counterparts, the poor stability of their absorber when humidity, oxygen, and/or light is present is the main issue impeding the long-term operation of PSCs and affecting their industrialization and commercialization. To address the stability issues and obtain significantly efficient and robust PSCs, a number of advanced strategies have been proposed in the literature, including optimization in terms of composition (cation–anion mixing, perovskite doping, and lead-free perovskite) and band-gap, additive, solvent/antisolvent, film deposition, and interface engineering [8,9]. In the last case, interface functionalization is realized through perovskite dimension (3D/0D, 3D/1D, and 3D/2D), molecular (dyes, polymers, etc.), ETL (SnO_2, PCBM, fullerene derivatives, sulfides, and metal doped-oxides), and HTM (spiro-OMeTAD replacement, NiOx, C-based PSCs, and other p-type materials) innovative engineering approaches [10–12]. This leads to appropriate energy-level alignment, minimal defects, and the development of highly hydrophobic interfaces with a high resistance to humidity attack. Justifying the high importance of interface functionalization for the development of highly significantly and robust devices, this review focuses on ETL/perovskite and perovskite/HTM interface engineering and encompasses the most recently proposed innovations with the purpose of optimizing the performance of PSCs.

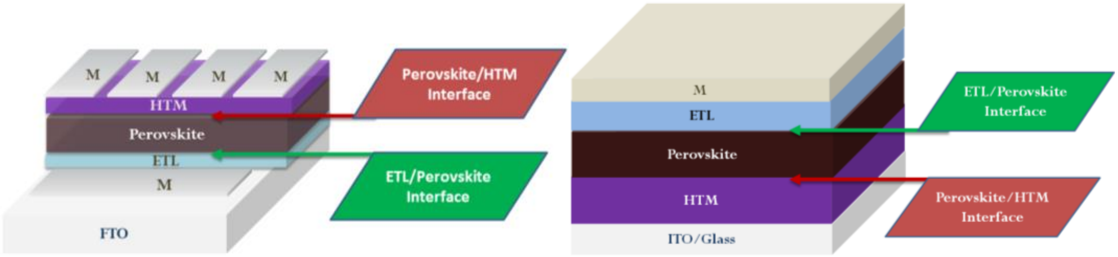

Figure 1. Schematic representation of conventional n-i-p (**left**) and inverted p-i-n (**right**) PSC architectures, depicting the functionalization of ETL/perovskite and perovskite /HTM interfaces (ETL: electron transport layer; HTM: hole transport material; M: Ag, Au, or Al metal contacts/charge collectors).

2. Functionalization of ETL/Perovskite Interface

The electron transport layer (ETL) plays a pivotal role in obtaining stable perovskite solar cells with a high power conversion efficiency (PCE) [13,14]. It must be characterized by high transparency to visible light, photostability, and compatibility with the perovskite used. Therefore, a thorough comprehension and optimization of the interaction between perovskite materials and TiO_2 ETL underlayers, as well as a special focus on the behavior of the corresponding devices, are necessary. Working toward this target, novel approaches based upon interface engineering in terms of functionalization of the electron transport layer (ETL) of perovskite solar cells (PSC) have recently been reported [15,16].

Transition metal semiconducting oxides (TMSO, e.g., TiO_2, SnO_2, ZnO, Zn_2SnO_4, CeO_2, Cr_2O_3, Fe_2O_3, and Nb_2O_5) [17] and fullerene derivatives (e.g., 6,6-phenyl-C61-butyric acid methyl ester/PCBM) [18–20] have been commonly employed as selective electron transport layers in PSCs. H.S. Kim et al. explored the addition of MXene/TMSO nanocomposites (MXenes: transition metal carbides, nitrides, or carbonitrides having a two-dimensional layered structure) to modify the PCBM ETL and further boosted the performance (PCE and long-term stability) of inverted perovskite solar cells (p-i-n PSCs) [21].

Inverted PSCs usually employ PCBM ([6,6]-phenyl-C61-butyric acid methyl ester) fullerene derivative as the ETL. However, the efficiency and lifespan of the corresponding devices are limited by a high degree of disorder and severe self-aggregation of the PCBM ETL. Working on inverted planar PSCs, Y. Jiang et al. used the chelation effect as a very useful tool to reduce the ETL disorder and, thus, enhance the efficiency and stability of the devices. The authors designed a series of functional dyads FP-Cn (n = 4, 8, 12), where fullerene and terpyridine chelating groups are linked via a flexible alkyl chain spacer. Using the FP-C8/C60 ETL dyad as the electron transport layer and $Cs_{0.05}FA_{0.90}MA_{0.05}PbI_{2.85}Br_{0.15}$ as the light absorber, PSCs with a PCE of 21.69%, minor hysteresis, good reproducibility, and high stability were obtained. By replacing perovskite with $FAPbI_3$, PSCs with the FP-C8/C60 ETL gave an optimal PCE of 23.08%, which is one of the highest efficiency values ever obtained with solution-processed fullerene derivatives [22].

In addition, following an interlayer strategy involving the in situ generation of polyethylenimine-based two-dimensional (2D) perovskite, C. Wang et al. boosted the efficiency, stability, and reproducibility of inverted planar perovskite solar cells by effectively reducing the lattice match between the NiOx HTL and the $MAPbI_3$ absorber, thereby suppressing the interfacial defect formation and developing perovskite layers with a high crystalline quality [23]. Moreover, working on FTO/NiOx/$MAPbI_3$/PC61BM/BCP/Ag

PSCs, I-H. Ho et al. modified the HTL/absorber interface with quaternary ammonium halide-containing cellulose derivatives and succeeded in producing perovskite films of high crystalline quality with large grains, low surface roughness, enhanced light absorption, and increased hole mobility. The coating with cellulose polymeric materials smoothens the NiO_x HTL surface, tunes its wettability, improves the compatibility with the perovskite absorber, and passivates uncoordinated Pb^{2+} species. As a result, the $MAPbI_3$-based inverted PSCs modified by cellulose polymers showed improved photovoltaic performance and high stability after storage under ambient conditions [24].

Taking the advantage that perovskite solar cells are considered the evolution of dye-sensitized solar cell technology, the idea of dye sensitization for optimizing the ETL/perovskite interface was investigated by N. Balis et al. [25]. The use of the solution-processable D35 [triphenylamine-based metal-free (E)-3-(5-(4-(bis(2′,4′-dibutoxy-[1,1′-biphenyl]-4-yl) amino) phenyl) thiophen-2-yl)-2-cyanoacrylic acid] D-π-A organic chromophore to sensitize the TiO_2 compact layer (Figure 2) led to planar PSCs based on $MAPbI_3$ achieving a power conversion efficiency of 17% (against 15% of those with a non-sensitized layer), which was accompanied by further improved stability. The obtained results suggest that this performance improvement can be attributed to enhanced recombination resistance, increased electron transport, better crystallization of the deposited perovskite, defect passivation, roughness reduction, dipole moment effects, and the humidity sealing character of the hydrophobic dye monolayer. Thus, for the first time in the literature, it was demonstrated that dye sensitization could be effectively applied to interface engineering in PSCs.

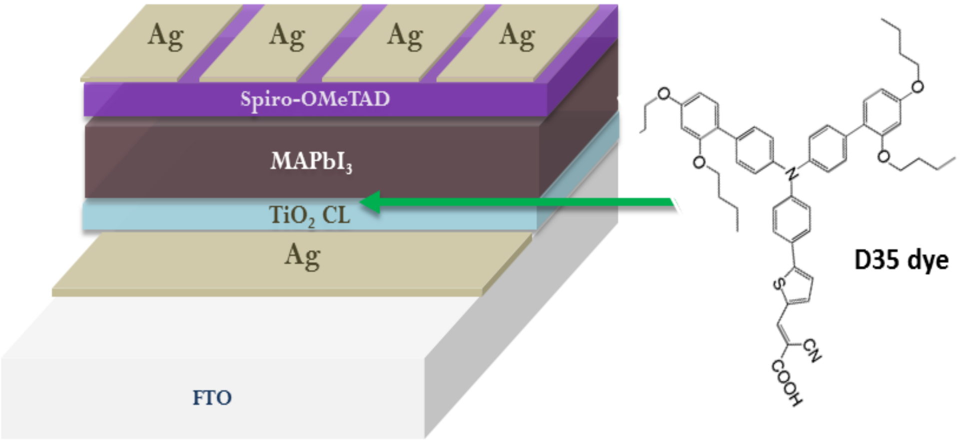

Figure 2. Functionalization of the $TiO_2/MAPbI_3$ interface following sensitization of the TiO_2 compact layer (CL) by the hydrophobic D35 dye.

PSCs' instability remains the most significant issue preventing them from industrial scaling up. In this context, the dye-sensitization approach was expanded by investigating its effect on the stability of planar PSCs against thermal and light stresses [26]. The stability investigation showed an improved endurance of devices after the insertion of D35 under shelf-shield conditions and especially after accelerated thermal treatment (retaining almost 80% of their initial efficiency after 60 min at 100 °C) and prolonged light saturation exposure (low degradation following continuous illumination for 7 h at 76.5 $mWcm^{-2}$ incident irradiance in the 300–800 nm spectral range). This study confirmed the plethoric role of the dye-sensitization approach and the advantages it confers to interfacial engineering via organic chromophores for achieving efficient and stable PSCs. Further developments are expected as the dye-sensitization methodology can further employ a large number of molecular hydrophobic dyes, disposing exceptional structural and optoelectronic properties.

The effect of dye modification on TiO_2 and ZnO electron transport layers in planar PSCs was also reported by R. Chouk et al. [27]. As a sensitizer, the authors employed a Schiff base–cobalt complex derived from ninhydrin and glycine ligands and succeeded in improving the photoinduced electron transfer and the resulting device efficiency and stability. The authors confirmed the existence of strong interactions between the Cobalt (II) dye and the ETLs and obtained a significant efficiency increase in the performance of the corresponding FTO/TiO_2/Co-NG/$MAPbI_3$/Spiro-OMeTAD/Ag and FTO/ZnO/Co-NG/$MAPbI_3$/Spiro-OMeTAD/Ag solar cells (equal to 18.94% and 16.32%, respectively).

Noh et al. [28] selected an electron-accepting n-type organic semiconductor [3,9-bis(2-metylene-(3-(1,1-dicyanomethylene)-indanone))-5,5,11,11-tetrakis(4-hexylphenyl)-dithieno [2,3-d:2′,3′-d′]-s-indaceno [1,2-b:5,6-b′] dithiophene/ITIC—Scheme 1a] to passivate the surface of SnO_2 and, thus, developed an organic/inorganic double ETL. The glass/ITO//PEIE-SnO_2-ITIC//$(FAPbI_3)_{0.95}(MAPbBr_3)_{0.05}$//Spiro-OMeTAD/Au planar architecture, incorporating the optimized ETL, presents improved energy band alignment, low contact resistance, reduced trap-state density, and reached PCE values exceeding 16% (with marginal hysteresis), which remained practically unchanged for 200 h.

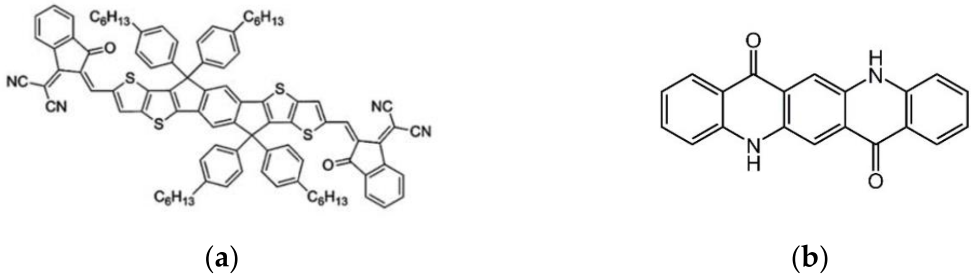
(**a**) (**b**)

Scheme 1. ITIC (**a**) and QA (**b**) molecular structures.

Molecular dyes can also be used to functionalize inverted architectures. Y. Qi et al. [29] designed novel organic cationic cyanine dye molecules and were able to efficiently passivate the interface between the PC61BM and Ag electrode in ITO/Glass//PTAA//perovskite//PCBM/Dye/Ag devices, improving the PCE from a value of 14.24% (control) to 19.14% (functionalized). The efficiency increase was attributed to reduced interface charge recombination and improved charge transport. The addition of the dye interlayer offered additional protection from moisture, and the corresponding devices maintained 90% of their initial PCE for 120 h (under ambient conditions).

In order to address the long-term stability issues of PSCs, Q. He et al. introduced a novel perovskite ($MAPbI_3$ and triple cation) surface passivation strategy involving quinacridone (QA—Scheme 1b) hydrophobic coating. The addition of such an insoluble, low-cost industrial organic pigment results in passivated glass/ITO//SnO_2//$MAPbI_3$//Spiro-OMeTAD//Au PSCs with considerably improved performance (PCE of 21.1% with low hysteresis) and notable stability (maintaining 85.7% of their initial PCE after 240 h of storage at 85 °C) [30].

A number of transition metal oxides and related compounds (including TiO_2 and perovskite oxides) have been successfully used as ETLs [31–41]. However, despite its extensive use as both a compact and a mesoporous layer, titanium dioxide (TiO_2) is characterized by low electron mobility and poor conductivity, and may act as a photocatalyst of chemical reactions, leading to the degradation of perovskites and permanent polarization of the film [42–45]. Innovative engineering strategies focusing on ETL/perovskite interface optimization are necessary to address the above issues. Metal (Y, Co, Li, Ag, Sn, Fe, Ru, Nb, Zn, Ta, or Mg) and non-metal (F, Cl, or S) doping have been proposed as effective ETL modification strategies that can lead to enhanced electrical conductivity, increased charge transport, and reduced charge recombination [46–66]. Furthermore, S.-H. Chen et al. synthesized mesoscopic Ag-doped TiO_2 (meso-Ag:TiO_2) to address the serious hysteresis problems encountered in planar structures. Thus, perovskite devices [FTO glass/dense TiO_2/meso-Ag:TiO_2/$CH_3NH_3PbI_3$/spiro-OMeTAD/Ag] incorporating a meso-Ag:TiO_2 ETL present low hysteresis, and their optimization results in a PCE as high as 17.7% [67]. On the other hand, the efficiency and stability of PSCs are sensitive to UV light, heat, and humidity, and strongly depend on the properties of ETLs. Transition metal oxides such as TiO_2 can trigger light instability due to photocatalysis [68]. Indeed, it has been recently demonstrated that the presence of a hygrophobic copper-modified TiO_2 ETL (Figure 3) primarily mitigates the photodegradation action of the substrate, boosts the perovskite nanomorphology, passivates the surface trap states of the perovskite absorber, and facilitates electron transport to the ITO charge collector [69]. The addition of Cu monovalent cations downshifts the Fermi level of TiO_2 and gives rise to a significant improvement in the performance of perovskite nanohybrids in terms of efficient energy conversion to electricity.

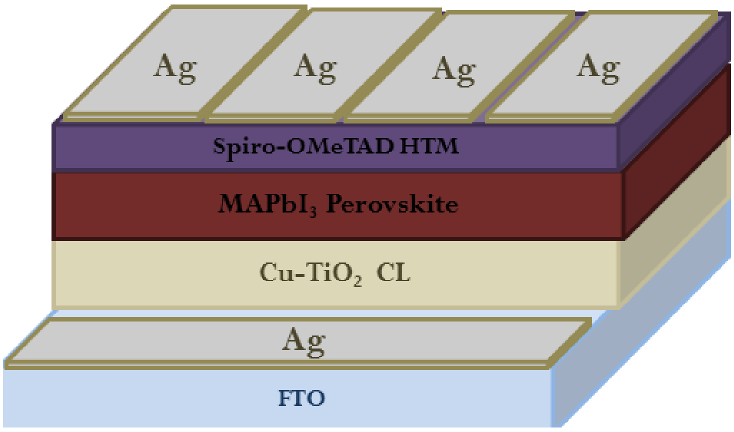

Figure 3. Architecture of a planar PSC device based on Cu-modified TiO_2 ETL.

Indeed, perovskite devices using a Cu-modified compact TiO_2 ETL present a PCE exceeding 18%, outperforming by more than 1% the corresponding efficiency of the reference device [69]. This work confirms the advantages of interface engineering via metal ion doping as a totally aspiring and novel strategy with multiple consequences in the field of PSCs. The above strategy can be employed to many photosensitive metal oxide ETL materials possessing suitable optoelectronic and structural characteristics with TiO_2, thus enabling the development of highly efficient and more robust energy systems (solar cells, LEDs, and FETs) against environmental stresses.

According to the literature, mesostructured devices are among the most efficient PSCs where titanium dioxide pastes are commonly employed to deposit compact and mesoporous ETLs. Graphitic carbon nitride (g-C_3N_4) is a very promising two-dimensional (2D) polymeric material for photovoltaic applications due to its good stability and suitable electronic properties (heat-resistant n-type semiconductor).

Z. Liu et al. employed n-type g-C_3N_4 ultrathin films to modify the ETL/perovskite and perovskite/HTL interfaces in planar PSCs, and despite a challenging band alignment, they achieved a PCE as high as 19.67% and long-term stability, which was attributed to the dramatically reduced trap density at the ETL/perovskite and perovskite/HTL interfaces [70]. In a recent contribution, it was demonstrated that the presence of a 2D g-C_3N_4 material on the surface of a mesoporous TiO_2 ETL (Figure 4 on the left) primarily results in the exact conduction band alignment of mp-TiO_2 and $CH_3NH_3PbI_3$ perovskite, thus enhancing the charge carrier transfer and minimizing the energy losses of the photogenerated excitons [71]. Furthermore, the conduction band alignment is extended until the FTO by substituting the widely used TiO_2 compact layer with an ultrathin ALD ZnO layer (Figure 4 on the right), and thus, the electron transport to the charge collector is further facilitated, achieving PCE values as high as 20.53%. Another significant aspect of this interface modification is the long-term stability of these devices, which can be attributed to the hydrophobic environment that g-C_3N_4 creates before the perovskite layer. As such, this gives rise to a substantial improvement in the performance of perovskite nanohybrids in terms of efficient energy conversion to electricity. This work confirms the advantages of interface engineering via 2D carbon-based materials as a totally aspiring and novel approach with multiple consequences in the field of PSCs. This strategy can be further exploited by investigating the impact of other 2D structures and nanocarbon composites.

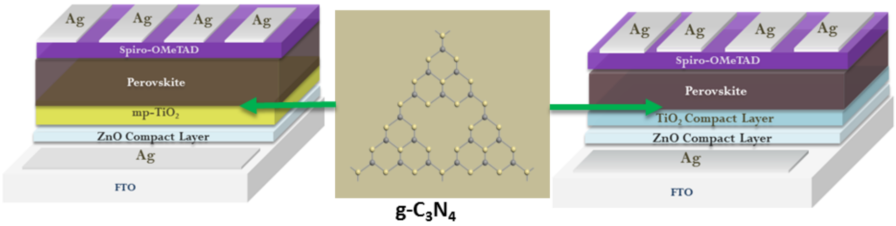

Figure 4. Functional incorporation of graphitic carbon nitride (g-C_3N_4) at the TiO_2/perovskite interface for planar (**left**) and mesostructured (**right**) PSCs.

3. Functionalization of Perovskite/HTM Interface

The hole transport material (HTM) used and especially its interface with the perovskite absorber also plays a pivotal role in obtaining PSCs with a high power conversion efficiency (PCE) and enhanced stability. Thus, advanced engineering methodologies have been developed, focusing on perovskite HTL/interface optimization and including the incorporation of polymers, semiconductors, metal oxides, and molecular materials (both organic and inorganic) [72–74] to regulate and refine the physicochemical properties and electronic levels of the interface between perovskite active layers and HTM materials.

Stable radical molecules disposing unpaired valence electrons and high electron acceptance–donation ability are excellent candidates for improving the performance of both perovskite absorber and charge transporting layers [75]. Indeed, to this direction, Q. Jiang et al. synthesized a donor–acceptor radical molecule combining an electron deficient para-diazine core with four methoxytriphenylamine electron-donating peripheral units. The novel PT-TPA molecule with a resonance structure is able to interact (take an electron) with perovskite, forming p-type doping accompanied by band bending. Thus, the corresponding ITO/SnO_2/$FA_{0.92}MA_{0.08}PbI_3$/PT-TPA/Spiro-OMeTAD/Ag PSCs incorporating the radical-doped interface delivered an efficiency of 23.4% [76].

In addition, a recent contribution reports on the use of 3,4-Bis(4-bromophenyl)cyclobut-3-ene-1,2-dione (BED) squaraine chromophore with a zwitterionic resonance structure to adjust the perovskite energy levels [77]. More precisely, it was demonstrated that the ortho-squaraine BED zwitterionic derivative is able modify the perovskite surface and lead to PSCs (Figure 5) achieving a PCE of 23.82%. Indeed, existing electron delocalization in the stabilized four-membered quadrupolar structure could result in p-type interaction with perovskite, involving intermolecular pairing between a single electron of BED and an electron in the absorber. This interaction is accompanied by surface doping and corresponding energy band reorganization, which leads to a significant increase in V_{oc}. Meanwhile, a threefold increase in hole mobility was observed, which is attributed to the formation of BED π-π stacking with the spiro-OMeTAD HTM and consistent with easier charge transfer. However, taking into account the importance of squaraine derivatives as interface modifiers, more significant developments are expected, targeting to the design and synthesis of novel resonant of π-conjugated squaraines with substituted peripheral phenyl groups, which are able to directly coordinate with Pb^{2+} through van der Waals forces.

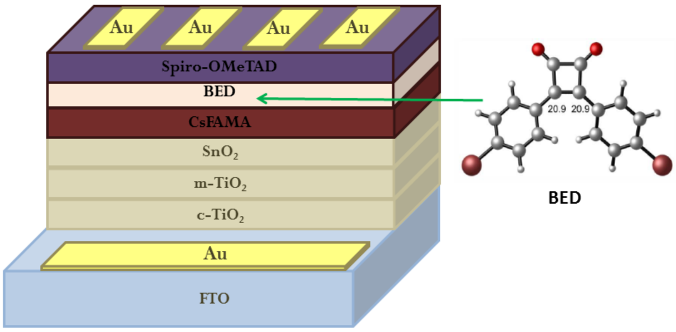

Figure 5. PSC architecture incorporating a BED squaraine derivative at the perovskite/HTM interface.

Graphene and graphene-based nanomaterials present excellent optoelectronic, photonic, thermal, and mechanical properties. They can be used to modify the transparent electrode, the absorber, the charge extracting layers, and the corresponding interfaces and address the stability, scalability, and flexibility challenges that limit the industrial applications of PSCs [78]. In particular, graphene oxide (GO) and reduced graphene oxide (rGO) are ideal candidates, being able to improve device performance in real working conditions. This is due to their outstanding optoelectronic properties, their high number of oxygen functionalities, and their large surface area, which affect the charge transport properties. In the literature, there are significant studies adopting graphene and graphene oxide in charge transport or perovskite layers with positive effects on the performance of the devices examined [79–83]. However, the works on graphene materials are fragmentary and further elucidation of their influence when added in PSCs is necessary. Thus, the effects of reduced graphene oxide (rGO)'s presence within the main components of a planar PSC (namely the compact electron transport layer, the perovskite absorber, and the hole transporter) was extensively investigated by N. Balis et al., who adopted a novel approach by combining an optimized rGO synthetic protocol with one-step perovskite layer deposition using lead acetate precursor [84]. Therefore, for the first time in the literature, high functionality in both the TiO_2 ETL and $MAPbI_3$ perovskite layers was obtained (Figure 6), resulting in significant performance enhancement of the PSCs under eximination. Consequently, the power conversion efficiency of the PSCs was improved by 20%, resulting in a ~14% stabilized power for the best rGO-containing device.

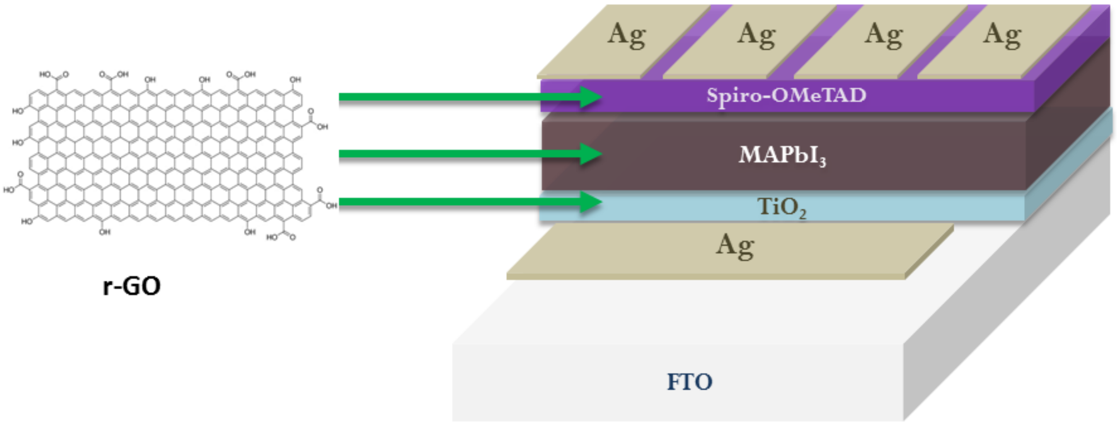

Figure 6. Incorporation of reduced graphene oxide (r-GO) into the main components of PSCs.

The contribution of rGO is significant not only by offering improved conductive pathways for charge carriers' transport, but also by favoring the growth of robust and homogenous perovskite layers, thus affecting the nanomorphology of the perovskite absorber. Therefore, the obtained results contribute significantly to a thorough comprehension of the interaction between perovskite materials and graphene derivatives, as well as the behavior of the corresponding devices. X. Lin et al. focused their efforts on the optimization of the rear electrode of PSCs by stabilizing a Cu-Ni alloy between two layers of graphene deposited by CVD. The composite alloy substrate improves the work function of copper and its electrochemical properties, acts as a buffer preventing its diffusion into the perovskite absorber, and presents increased resistance against humidity, heat, and oxygen. It, thus, results in devices with a PCE exceeding 24%, which remains practically stable for several months of continuous operation [85].

To avoid the decomposition of soft semiconducting hybrid perovskites, Y. Wang et al. proposed the formation of robust perovskite films in a stabilized heterostructure consisting of a perovskite surface rich in Pb and a chlorinated graphene oxide layer, characterized by the presence of strong Pb-Cl and Pb-O bonds in the crystalline structure. In addition to low recombination and high stability, this solid perovskite interface presents high selectivity for charge extraction and permits the fabrication of PSCs that are able to operate with an enhanced PCE at a high temperature for more than one month [86].

Moreover, graphene quantum dots (GQDs) were used by S. Pang et al. [87] to modify the SnO_2 ETL in perovskite solar cells. The performed modification results in strong electronic coupling and energy level matching at the perovskite/SnO_2 interface, leading to ITO/SnO_2:GQDs/$MAPbI_3Cl_{3-x}$/Spiro-OMeTAD/Ag devices with improved charge carrier extraction, suppressed charge recombination, and a high PCE of 21.1%.

PSCs' instability remains the most significant reason preventing them from industrial scaling up. Low-dimensional (LD) perovskites are primarily perceived as effective active materials for optoelectronic devices [88], and there are some interesting reports suggesting their incorporation in PV applications [89,90]. PSCs' stability can be significantly enhanced using dimensionality engineering strategies combining the 3D absorber with LD perovskites (0D, 1D, or 2D) [91]. Among them, sulfur-based perovskites and especially novel 1D materials based on organic trimethylsulfonium [$(CH_3)_3S^+$] cations present improved chemical stability in ambient conditions and show great application potential [92–97]. Looking for novel approaches for interface engineering in perovskite solar cells (PSCs), A. Kaltzoglou et al. expanded their research on the double perovskite approach by investigating the effect of tridimensional/monodimensional (3D/1D) perovskite bilayer consisting of (FA/MA/Cs)$PbI_{3-x}Br_x$ (3D) and $(CH_3)_3SPbI_3$ (1D) perovskites [98] on the stability of PSCs against humidity and light stresses (Figure 7).

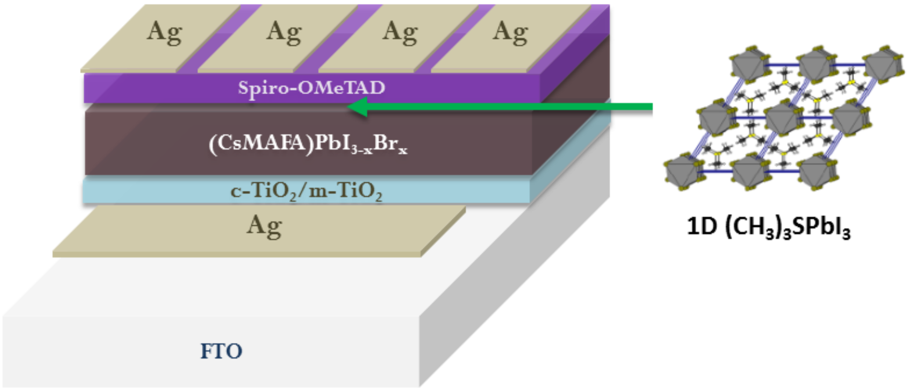

Figure 7. Interface functionalization of PSCs realized through a 3D/1D engineering strategy, involving the incorporation of 1D $(CH_3)_3SPbI_3$ perovskite between the main 3D absorber and the spiro-OMeTAD HTM. The perovskite/spiro-OMeTAD interface can also be appropriately altered to incorporate 3D/0D and 3D/2D structures.

One of the originalities of this work lies in its use of a two-perovskite dimensionality engineering strategy, which consists of interface optimization by adding an air-stable wide band-gap 1D perovskite layer on top of the main absorber. The devices based the 3D/1D bilayer show a significant reduction in charge carrier recombination, which is accompanied by high stability against humidity and light stresses. It is clear that dimensionality engineering employing 1D perovskite as a shield for water molecules and a promoter of charge carrier transporters in perovskite PV devices constitutes an extremely promising and novel approach with a significant impact in the relevant field. Contrary to other approaches, the additional perovskite (1D) layer creates a favorable environment that improves the action of the main perovskite absorbers in terms of stability improvement and performance reproducibility. On the other hand, M. Parashar et al. employed trimethylsulfoxonium ($TMSO^+$) aprotic cations and developed very stable PSCs with enhanced performance and moisture resistance. Their behavior was attributed to the ability of $TMSO^+$ cation to interact with Pb^{2+}, forming a dative Pb-O bond in a separate 1-D structure. The glass/FTO/TiO_2/$(TMSOPbI_3)_x(MAPbI_3)_{100-x}$/spiro-OMeTAD/Au devices containing the fused, highly hydrophobic 1-D/3-D $(TMSOPbI_3)_x(MAPbI_3)_{100-x}$ perovskite achieved a PCE of 19.94%, together with V_{OC} values exceeding 1.12 V [99].

Poor stability of the perovskite layer is an important issue usually related to ionic defects on the absorber surface acting as charge recombination sites and water/oxygen infiltration positions. The incorporation of organic compounds with oxygen functional groups (e.g., carbonyls and carboxyls) has been proposed as an effective tool to passivate perovskite structural imperfections and improve device stability [100–106]. To address the efficiency and stability challenges encountered in PSCs, the perovskite/hole transporter interface was optimized using a multifunctional layer consisting of D35 organic dye (Figure 8). The presence of the hydrophobic D-π-A interlayer mainly boosts the perovskite nanomorphology, facilitates the hole transport to the cathode via appropriate energy-level alignment, and passivates the surface trap states of the perovskite absorber. As a result, this leads to a substantial improvement in the performance of $(FA/MA/Cs)PbI_{3-x}Br_x$ nanohybrids in PSCs, showing efficient energy conversion to electricity with a PCE of 18.5% [107] and presenting high stability for several weeks after storage in the dark for several weeks (with no bias).

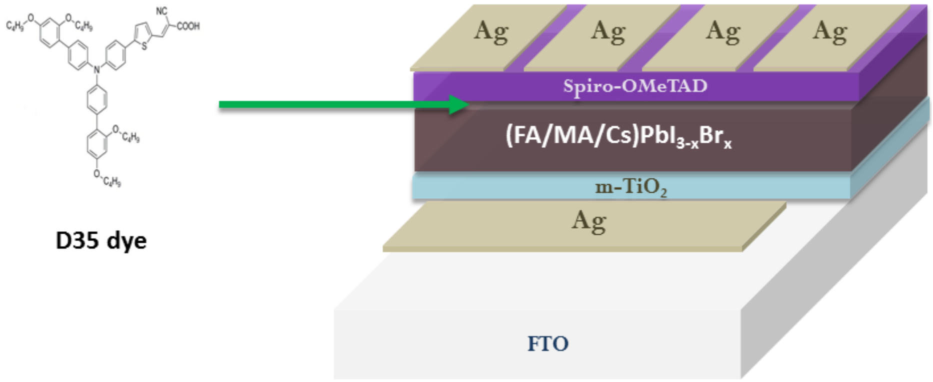

Figure 8. Incorporation of D35 chromophore at the perovskite/Spiro-OMeTAD interface.

Tian Zhang et al. designed and synthesized 4-(5-(7-(5-(5,11-bis(2-ethylhexyl)- 5,11-dihydroindolo[3,2-b]carbazol-2-yl)-4-hexylthiophen-2-yl)benzo[c][1,2,5]thia diazol-4-yl)-3-hexylthiophen-2-yl)benzoic acid (ZT001) donor–π–acceptor molecular dye and employed it to mitigate surface defects and water-sensitivity problems. The D–π–A organic dye disposes long alkyl hydrophobic chains and carboxyl groups, which coordinate with Pb^{2+} species. This leads to considerable reduction in the structural defects and passivation of the perovskite films. The ZT001-modified FTOGlass//$SnO_2/Cs_{0.05}$ $(FAPbI_3)_{0.85}(MAPbBr_3)_{0.15}$/ZT001/spiro-OMeTAD/Au device exhibited a PCE of 20.6%, along with a high V_{OC} and a large fill factor (FF) as well as improved resistance under humid conditions [108]. These works confirm the advantage of using functional molecular chromophores as a very ambitious and innovative novel interface engineering strategy that can further benefit from a variety of photosensitive materials with a suitable structure and appropriate optoelectronic properties.

Significant PCE enhancement in the field of PSCs has been achieved using mixed-cation perovskite films. However, these composite hybrid materials suffer from inherent instability due to the presence of multiple defects, including halide (I, Br) vacancies or uncoordinated Pb^{2+} sites developed during the deposition of the absorber layer. Thus, destruction of PbX6 octahedral might occur under humid operational conditions, which is usually accompanied by poor stability and progressive efficiency decline of the corresponding devices [109–113].

In order to improve waterproof performance, 1-Dodecanethiol (DDT) was used to passivate the surface and provide perovskite films with high hydrophobicity. This work focused on the most known mixed-cation perovskite formulation, $(FAPbI_3)_{0.85}(MAPbBr_3)_{0.15}$, which is targeted to repair defects and improve moisture resistance of the absorber. Through a series of tests, it was found that perovskite defects repaired by the thiol group in DDT (Figure 9) could reduce trap density, inhibit non-radiative recombination, and improve charge carrier transportation and extraction performance.

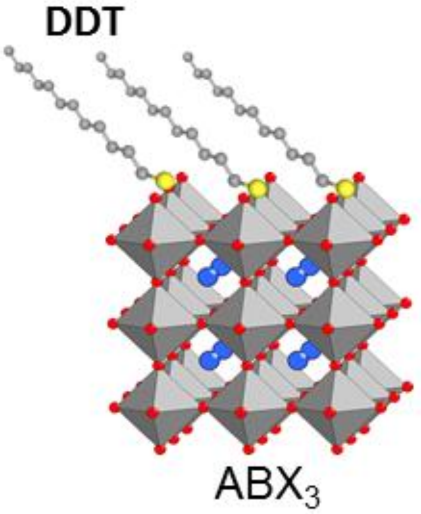

Figure 9. Perovskite passivation by hydrophobic 1-Dodecanethiol (DDT).

In addition, a significant improvement was observed in the device performance (in terms of efficiency and stability), which was attributed to the existence of highly hydrophobic dodecyl organic groups in the DDT modifier. Accordingly, following post-treatment with DDT, a PCE value of 20.89% was obtained, together with exceptional long-term stability (exceeding 90%) after storage under humid conditions for more than 40 days [114]. These very promising results confirm the high potential of using thiol-functionalized molecules for repairing perovskite structural defects and justify the necessity of coordinated and intensive research in the field with high prospects of practical implementation.

Functional electron-rich sulfur containing small molecules has also been used as an interfacial passivator to coordinate Pb atoms. D.A. Kara et al. introduced 2-thiophenecarboxylic acid (2TiCOOH) as a passivation interlayer between perovskite and spiro-OMeTAD HTM by spin coating a solution of 2TiCOOH in chlorobenzene (CB) on the top surface of the absorber. The modified $FTO/TiO_2/Cs_{0.05}(FA_{0.83}MA_{0.17})_{0.95}Pb(I_{0.83}Br_{0.17})_3$/2TiCOOH/spiro-OMeTAD/$MoO_3$/Ag devices with an n–i–p planar architecture present high carrier lifetime, easy charge extraction, and low recombination, together with enhanced photovoltaic parameters and extremely stable operation for more than 100 days [115].

The long-term instability of PSCs restricts their scaling up for commercialization. To alleviate this very challenging issue, the development of devices with self-healing properties and improved resistance against humidity has been proposed [116–121]. Very recently, Y. Niu et al. introduced polyvinylpyrrolidone (PVP) to a methylammonium lead iodide ($MAPbI_3$) perovskite precursor in order to control crystal growth and endow such devices with self-healing ability in a humid environment [122]. The nuclear magnetic resonance measurements confirmed the existence of strong hydrogen bonding interaction between PVP and $MAPbI_3$ (Figure 10). As a result, a compact perovskite film with excellent electronic, morphological, and structural quality was formed, leading to PSCs with a power conversion efficiency (PCE) of up to 20.32%.

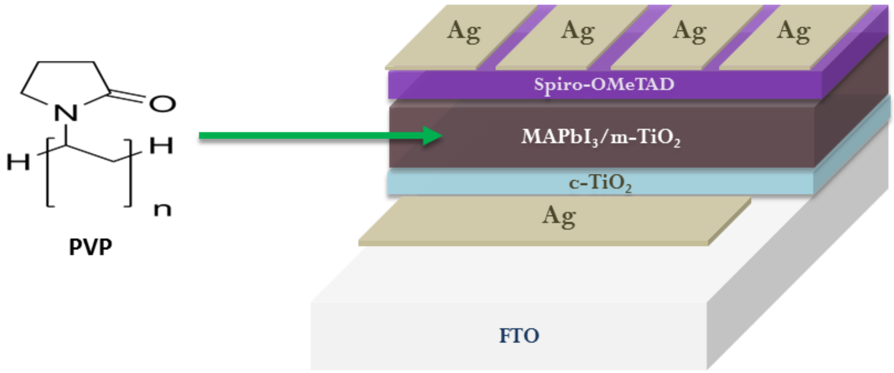

Figure 10. PSC architecture based on functional incorporation of polyvinylpyrrolidone (PVP) in the perovskite precursor.

In addition, $CH_3NH_3^+$ cation decomposition was suppressed and $MAPbI_3$ recrystallization was improved due to the existence of hydrogen bonds at the grain boundaries. The corresponding PVP-modified devices exhibit remarkable resistance to moisture attack, with a slight efficiency decline following operation for 20 days under conditions of high humidity. This behavior is directly related to the excellent self-healing behavior of the perovskite layer following PVP introduction, which is characterized by slow crystal growth and low number of trap states.

Focusing on polymers, Y. Jing et al. synthesized fully conjugated porous aromatic frameworks (PAFs) having a stable tetraphenylene and pyrene backbone bridged by C=C. Polymeric materials with a high surface area were successfully applied to dope the perovskite absorber, acting as an efficient nucleation template and regulating perovskite crystallinity. As a result, the corresponding ITO/SnO_2/$Cs_{0.05}FA_{0.8}MA_{0.15}PbI_{2.55}Br_{0.45}$ + PAF/Spiro-OMeTAD/Ag uncapsulated devices showed improved performance with an optimal PCE of 22.76 %, suppressed hysteresis, and high stability for at least half a year under ambient conditions [123].

A polymer-based additive engineering approach was also used by Yang-Yen Yu et al. in inverted ITO/NiO_x/$CH_3NH_3PbI_3$/PC61BM/BCP/Ag p-i-n PSCs. The authors confirmed that functional groups in polyamic acid and polyimide could strongly interact with Pb^{2+} and $CH_3NH_3^+$ cations to passivate perovskite grain boundary defects. Following the addition of polymers, the grain size in the modified absorbers increased and the corresponding devices showed improved performance, which was accompanied with exceptional stability after storage under controlled conditions [124].

Despite significant progress, there is a lack of understanding about the underlying physical phenomena and chemistry of PSCs and the corresponding processes that determine the formation and stability of the perovskite absorber, the size and shape of perovskite crystals, the presence of defects, and the charge recombination and transport. There are significant research efforts in the literature to overcome the deficiency that could limit the ability to optimize device performance and improve device stability and lifetime. Indeed, Lewis acid and base adducts, dye sensitizers, crystal growth control, and organic compounds with multidentate groups have been employed for the successful modification of perovskite absorbers. Moreover, machine learning (ML) methods have been used to gain valuable insights from experimental data and to predict the structural and optoelectronic properties of the most promising materials for PSCs [125–135].

Inspired by recent developments in the field using functional chromophores, very recently, M. Elsenety et al. investigated an efficient and highly hydrophobic triphenylamine organic compound as an interlayer between the 3D perovskite absorber and the common Spiro-OMeTAD HTM, thus proposing a new route to fabricate highly efficient and thermally stable PSCs (Figure 11). The importance of the proposed strategy lies in the fact that triphenylamine molecules can further substitute triphemylamine derivatives, thus taking a significant step forward by designing and synthesizing novel passivating agents and increasing their application potential. In their study, DN-F10 ultra-hydrophobic triphenylphosphine derivative with a D-π-A structure was employed to form strong p-type interaction on the surface of perovskite and promote the fine tuning of energy levels, thus leading to devices with PCE values close to 21% [136].

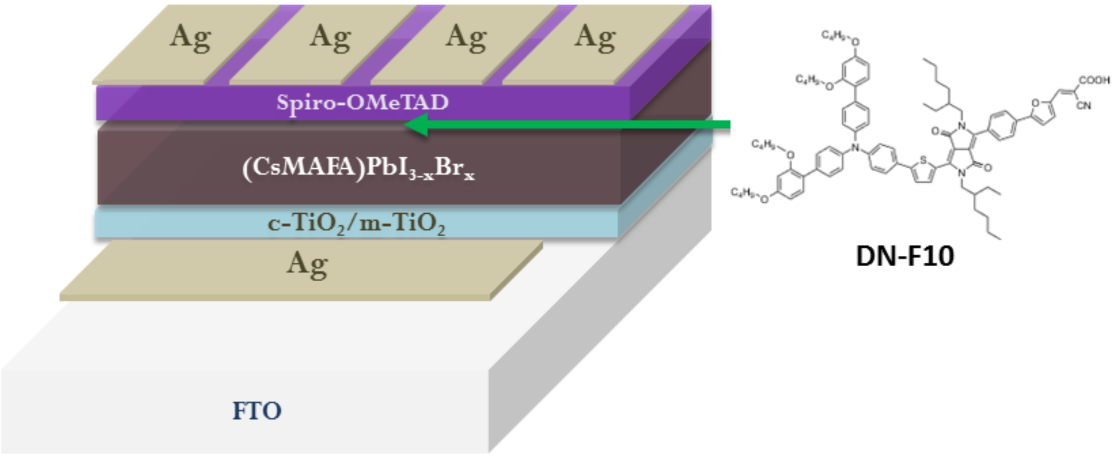

Figure 11. Modification of the perovskite/spiro-OMeTAD interface via functionalization with DN-F10 ultra-hydrophobic triphenylphosphine derivative.

The high values of the cell parameters were attributed to improved crystallization of perovskite and to the effective passivation of uncoordinated Pb^{2+} by the carboxyl groups of the DN-F10 dye. This interaction also affects the growth activation energy and decreases the crystallization rate, producing larger perovskite without significant defects. Meanwhile, due to the passivation effect, hole extraction at the perovskite/spiro-OMeTAD interface was enhanced and the charge carriers' recombination was suppressed, thus increasing the power conversion efficiency. Moreover, the terminal organic chains of DN-F10 endow the interface with an ultra-hydrophobic character, shielding perovskite from moisture while alleviating ionic diffusion, thus leading to excellent device stability. Furthermore, statistical analysis and machine learning (ML) modeling further confirmed the significance of the proposed innovative approach by identifying correlations between the photovoltaic parameters and predicting the coefficients of determination. In parallel, the ML models were able to suggest the relative significance of cell parameters to optimize device performance and accurately predict the corresponding PCE. Taking into account the plethora of functional groups able to interact with both the absorber and the corresponding charge transporting layers, we anticipate the employment of machine learning approaches to optimize molecular structures for interface engineering strategies and achieve PCEs exceeding 26% [137].

Indeed, in a very recent study, L. Zhang et al. [138] further elaborated the dye-modification approach by using machine learning and symbolic regression methods to discover the most appropriate organic interlayers, leading to optimized $MAPbI_3/TiO_2$ interfaces in hostile aqueous conditions. The authors were able to model and predict enhanced photovoltage and stability in water, achieving in parallel to experimentally validate with success their findings for a champion system comprising two molecular dyes. This work highlights the importance and the high potential of ML platforms to accelerate the design of functional interfaces, enabling the development of efficient and robust devices and their long-term operation in extreme environmental conditions.

4. Conclusions and Perspectives (and Future Directions)

Despite the spectacular enhancement in photovoltaic performance, device stability remains a key issue preventing the commercialization of PSCs. This work confirms that the functionalization of ETL/perovskite and perovskite/HTM interfaces results in perovskite layers with a low intrinsic defect density and balanced energy-level alignment that facilitates charge extraction. Previous research has demonstrated that dyes and functional chromophores with a D-π-A structure, polymers, transition metals, graphene oxides, and 2D carbon materials, as well as resonant molecules and 1D perovskites, are ideal candidates for interface modification, which can inhibit the degradation of the light absorber and ensure the robustness of PSCs. Following these innovative functionalization approaches, the PCE of the corresponding devices considerably increases and reaches very high values (from 15% for non-modified cells to almost 24% for interface-modified ones). Finally, it has been proven that validation of experimental results is possible by combining machine learning and autonomous experimentation, which leads to a better knowledge of the correlations between photovoltaic parameters and permits the determination of their optimized values. In parallel, ML offers the possibility of developing models for accurate prediction of cell performance, thereby speeding up the development of highly efficient practical devices. Significant progress toward industrialization can be expected in terms of both performance and stability by introducing all these innovative interface engineering strategies supported by advanced ML procedures in scale-up protocols (including also tandem devices), in combination with appropriate encapsulation and innovative sealing materials.

Author Contributions: Conceptualization, C.F.; methodology, C.F. and E.S.; validation, C.F. and E.S.; formal analysis, C.F. and E.S.; investigation, C.F. and E.S.; resources, C.F. and E.S.; data curation, C.F. and E.S.; writing—original draft preparation, C.F.; writing—review and editing, C.F. and E.S.; visualization, C.F.; supervision, E.S.; project administration, E.S.; funding acquisition, E.S. All authors have read and agreed to the published version of the manuscript.

Funding: This research was funded by the Hellenic Foundation for Research and Innovation (H.F.R.I.) under the “2nd Call for H.F.R.I. Research Projects” (PVLumo-project number 3730).

Data Availability Statement: Not applicable.

Conflicts of Interest: The authors declare no conflict of interest. The funders had no role in the design of the study; in the collection, analyses, or interpretation of data; in the writing of the manuscript; or in the decision to publish the results.

References

1. Saliba, M.; Matsui, T.; Domanski, K.; Seo, J.-Y.; Ummadisingu, A.; Zakeeruddin, S.M.; Correa-Baena, J.-P.; Tress, W.R.; Abate, A.; Hagfeldt, A.; et al. Incorporation of rubidium cations into perovskite solar cells improves photovoltaic performance. *Science* **2016**, *354*, 206–209. [CrossRef] [PubMed]
2. Li, Z.; Li, B.; Wu, X.; Sheppard, S.A.; Zhang, S.; Gao, D.; Long, N.J.; Zhu, Z. Organometallic-Functionalized Interfaces for Highly Efficient Inverted Perovskite Solar Cells. *Science* **2022**, *376*, 416–420. [CrossRef]
3. Chen, C.-I.; Wu, S.; Lu, Y.-A.; Lee, C.-C.; Ho, K.-C.; Zhu, Z.; Chen, W.-C.; Chueh, C.-C. Enhanced Near-Infrared Photoresponse of Inverted Perovskite Solar Cells Through Rational Design of Bulk-Heterojunction Electron-Transporting Layers. *Adv. Sci.* **2019**, *6*, 1901714. [CrossRef] [PubMed]
4. Rong, Y.; Hu, Y.; Mei, A.; Tan, H.; Saidaminov, M.I.; Seok, S.I.; McGehee, M.D.; Sargent, E.H.; Han, H. Challenges for Commercializing Perovskite Solar Cells. *Science* **2018**, *361*, 1214. [CrossRef] [PubMed]
5. Correa-Baena, J.P.; Saliba, M.; Buonassisi, T.; Grätzel, M.; Abate, A.; Tress, W.; Hagfeldt, A. Promises and Challenges of Perovskite Solar Cells. *Science* **2017**, *358*, 739–744. [CrossRef]
6. Stranks, S.; Snaith, H.J. Metal-halide perovskites for photovoltaic and light-emitting devices. *Nat. Nanotechnol.* **2015**, *10*, 391–402. [CrossRef]
7. Zheng, X.; Chen, B.; Dai, J.; Fang, Y.; Bai, Y.; Lin, Y.; Wei, H.; Zeng, X.C.; Huang, J. Defect passivation in hybrid perovskite solar cells using quaternary ammonium halide anions and cations. *Nat. Energy* **2017**, *2*, 17102. [CrossRef]
8. Chen, J.; Park, N.-G. Materials and Methods for Interface Engineering toward Stable and Efficient Perovskite Solar Cells. *ACS Energy Lett.* **2020**, *5*, 2742–2786. [CrossRef]
9. Shao, Y.; Yuan, Y.; Huang, J. Correlation of energy disorder and open-circuit voltage in hybrid perovskite solar cells. *Nat. Energy* **2016**, *1*, 15001–15006. [CrossRef]
10. Bu, T.; Li, J.; Zheng, F.; Chen, W.; Wen, X.; Ku, Z.; Peng, Y.; Zhong, J.; Cheng, Y.-B.; Huang, F. Universal passivation strategy to slot-die printed SnO_2 for hysteresis-free efficient flexible perovskite solar module. *Nat. Commun.* **2018**, *9*, 4609. [CrossRef]
11. Yang, D.; Yang, R.; Wang, K.; Wu, C.; Zhu, X.; Feng, J.; Ren, X.; Fang, G.; Priya, S.; Liu, S.F. High efficiency planar-type perovskite solar cells with negligible hysteresis using EDTA-complexed SnO_2. *Nat. Commun.* **2018**, *9*, 3239. [CrossRef] [PubMed]
12. Yun, A.J.; Kim, J.; Hwang, T.; Park, B. Origins of Efficient Perovskite Solar Cells with Low-Temperature Processed SnO_2 Electron Transport Layer. *ACS Appl. Energy Mater.* **2019**, *2*, 3554–3560. [CrossRef]

13. Luo, D.; Yang, W.; Wang, Z.; Sadhanala, A.; Hu, Q.; Su, R.; Shivanna, R.; Trindade, G.F.; Watts, J.F.; Xu, Z.; et al. Enhanced photovoltage for inverted planar heterojunction perovskite solar cells. *Science* **2018**, *360*, 1442–1446. [CrossRef]
14. Raiford, J.A.; Belisle, R.A.; Bush, K.A.; Prasanna, R.; Palmstrom, A.F.; McGehee, M.D.; Bent, S.F. Atomic layer deposition of vanadium oxide to reduce parasitic absorption and improve stability in n–i–p perovskite solar cells for tandems. *Sustain. Energy Fuels* **2019**, *3*, 1517–1525. [CrossRef]
15. Kamat, P.V.; Kuno, M. Halide Ion Migration in Perovskite Nanocrystals and Nanostructures. *Acc. Chem. Res.* **2021**, *54*, 520–531. [CrossRef]
16. Ricciarelli, D.; Kaiser, W.; Mosconi, E.; Wiktor, J.; Ashraf, M.W.; Malavasi, L.; Ambrosio, F.; De Angelis, F. Reaction Mechanism of Photocatalytic Hydrogen Production at Water/Tin Halide Perovskite Interfaces. *ACS Energy Lett.* **2022**, *7*, 1308–1315. [CrossRef]
17. Shin, S.S.; Lee, S.J.; Seok, S.I. Metal Oxide Charge Transport Layers for Efficient and Stable Perovskite Solar Cells. *Adv. Funct. Mater.* **2019**, *29*, 1900455. [CrossRef]
18. Xing, G.; Wu, B.; Chen, S.; Chua, J.; Yantara, N.; Mhaisalkar, S.; Mathews, N.; Sum, T.C. Interfacial Electron Transfer Barrier at Compact $TiO_2/CH_3NH_3PbI_3$ Heterojunction. *Small* **2015**, *11*, 3606. [CrossRef]
19. Jung, K.; Lee, J.; Im, C.; Do, J.; Kim, J.; Chae, W.-S.; Lee, M.-J. Highly Efficient Amorphous Zn_2SnO_4 Electron-Selective Layers Yielding over 20% Efficiency in $FAMAPbI_3$-Based Planar Solar Cells. *ACS Energy Lett.* **2018**, *3*, 2410–2417. [CrossRef]
20. Zhong, Y.; Hufnagel, M.; Thelakkat, M.; Li, C.; Huettner, S. Role of PCBM in the Suppression of Hysteresis in Perovskite Solar Cells. *Adv. Funct. Mater.* **2020**, *30*, 1908920. [CrossRef]
21. Hussain, S.; Liu, H.L.; Vikraman, D.; Jaffery, S.H.A.; Nazir, G.; Shahzad, F.; Batoo, K.M.; Jung, J.W.; Kang, J.W.; Kim, H.-S. Tuning of electron transport layers using MXene/metal-oxide nanocomposites for perovskite solar cells and X-ray detectors. *Nanoscale* **2023**, *15*, 7329–7343. [CrossRef] [PubMed]
22. Jiang, Y.; Wang, J.; Zai, H.; Ni, D.; Wang, J.; Xue, P.; Li, N.; Jia, B.; Lu, H.; Zhang, Y.; et al. Reducing Energy Disorder in Perovskite Solar Cells by Chelation. *J. Am. Chem. Soc.* **2022**, *144*, 5400–5410. [CrossRef] [PubMed]
23. Wang, C.; Yang, H.; Xia, X.; Wang, X.; Li, F. Suppressing interfacial defect formation derived from in-situ-generated polyethylenimine-based 2D perovskites to boost the efficiency and stability NiO_x-based inverted planar perovskite solar cells. *Appl. Surf. Sci.* **2021**, *548*, 149276. [CrossRef]
24. Ho, I.-H.; Huang, Y.-J.; Cai, C.-E.; Liu, B.-T.; Wu, T.-M.; Lee, R.-H. Enhanced Photovoltaic Performance of Inverted Perovskite Solar Cells through Surface Modification of $aNiO_x$-Based Hole-Transporting Layer with Quaternary Ammonium Halide–Containing Cellulose Derivatives. *Polymers* **2023**, *15*, 437. [CrossRef]
25. Balis, N.; Zaky, A.A.; Perganti, D.; Kaltzoglou, A.; Sygellou, L.; Katsaros, F.; Stergiopoulos, T.; Kontos, A.G.; Falaras, P. Dye Sensitization of Titania Compact Layer for Efficient and Stable Perovskite Solar Cells. *ACS Appl. Energy Mater.* **2018**, *1*, 6161–6171. [CrossRef]
26. Zaky, A.A.; Balis, N.; Gkini, K.; Athanasekou, C.; Kaltzoglou, A.; Stergiopoulos, T.; Falaras, P. Dye Engineered Perovskite Solar Cells under Accelerated Thermal Stress and Prolonged Light Exposure. *ChemistrySelect* **2020**, *5*, 4454–4462. [CrossRef]
27. Chouk, R.; Haouanoh, D.; Aguir, C.; Bergaoui, M.; Toubane, M.; Bensouici, F.; Tala-Ighil, R.; Erto, A.; Khalfaoui, M. Dye Sensitized TiO_2 and ZnO Charge Transport Layers for Efficient Planar Perovskite Solar Cells: Experimental and DFT Insights. *J. Electron. Mater.* **2020**, *49*, 1396–1403. [CrossRef]
28. Noh, Y.W.; Lee, J.H.; Jin, I.S.; Park, S.H.; Jung, J.W. Enhanced efficiency and ambient stability of planar heterojunction perovskite solar cells by using organic-inorganic double layer electron transporting material. *Electrochim. Acta* **2019**, *294*, 337–344. [CrossRef]
29. Qi, Y.; Ndaleh, D.; Meador, W.E.; Delcamp, J.H.; Hill, G.; Pradhan, N.R.; Dai, Q. Interface Passivation of Inverted Perovskite Solar Cells by Dye Molecules. *ACS Appl. Energy Mater.* **2021**, *4*, 9525–9533. [CrossRef]
30. He, Q.; Worku, M.; Liu, H.; Lochner, E.; Robb, A.J.; Lteif, S.; Raaj, J.S.; Winfred, V.; Hanson, K.; Schlenoff, J.B.; et al. Highly Efficient and Stable Perovskite Solar Cells Enabled by Low Cost Industrial Organic Pigment. *Angew. Chem. Int. Ed.* **2021**, *60*, 2485. [CrossRef]
31. Mahmud, M.A.; Elumalai, N.K.; Upama, M.B.; Wang, D.; Ales, V.G. Cesium compounds as interface modifiers for stable and efficient perovskite solar cells. *Sol. Energy Mater. Sol. Cells* **2018**, *174*, 172–186. [CrossRef]
32. Ruankham, P.; Wongratanaphisan, D.; Gardchareon, A.; Phadungdhitidhada, S.; Choopun, S.; Sagawa, T. Full coverage of perovskite layer onto ZnO nanorods via a modified sequential two-step deposition method for efficiency enhancement in perovskite solar cells. *Appl. Surf. Sci.* **2017**, *410*, 393–400. [CrossRef]
33. Zhang, P.; Wu, J.; Zhang, T.; Wang, Y.; Liu, D.; Chen, H.; Ji, L.; Liu, C.; Ahmad, W.; Chen, Z.D.; et al. Perovskite solar cells with ZnO electron-transporting materials. *Adv. Mater.* **2018**, *30*, 1703737. [CrossRef] [PubMed]
34. Huang, A.; Lei, L.; Zhu, J.; Yu, Y.; Liu, Y.; Yang, S.; Bao, S.; Jin, P. Controllable deposition of TiO_2 nanopillars at room temperature for high performance perovskite solar cells with suppressed hysteresis. *Sol. Energy Mater. Sol. Cells* **2017**, *168*, 172–182. [CrossRef]
35. Huang, X.; Hu, Z.; Xu, J.; Wang, P.; Wang, L.; Zhang, J.; Zhu, Y. Low-temperature processed SnO_2 compact layer by incorporating TiO_2 layer toward efficient planar heterojunction perovskite solar cells. *Sol. Energy Mater. Sol. Cells* **2017**, *164*, 87–92. [CrossRef]
36. Ren, X.; Yang, D.; Yang, Z.; Feng, J.; Zhu, X. Solution-processed Nb: SnO_2 electron transport layer for efficient planar perovskite solar cells. *ACS Appl. Mater. Interfaces* **2017**, *9*, 2421–2429. [CrossRef]
37. Song, J.; Zheng, E.; Bian, J.; Wang, X.; Tian, W.; Sanehira, Y.; Miyasaka, T. Low temperature SnO_2-based electron selective contact for efficient and stable perovskite solar cells. *J. Mater. Chem. A.* **2015**, *3*, 10837–10844. [CrossRef]

38. Eze, V.O.; Seike, Y.; Mori, T. Efficient planar perovskite solar cells using solution processed amorphous WOx/fullerene C60 as electron extraction layers. *Org. Electron.* **2017**, *46*, 253–262. [CrossRef]
39. Pintilie, I.; Stancu, V.; Tomulescu, A.; Radu, R.; Besleaga Stan, C.; Trinca, L.; Pintilie, L. Properties of perovskite ferroelectrics deposited on F doped SnO_2 electrodes and the prospect of their integration into perovskite solar cells. *Mater. Des.* **2017**, *135*, 112–121. [CrossRef]
40. Eperon, G.E.; Burlakov, V.M.; Docampo, P.; Goriely, A.; Snaith, H.J. Morphological Control for High Performance, Solution Processed Planar Heterojunction Perovskite Solar Cells. *Adv. Funct. Mater.* **2014**, *24*, 151–157. [CrossRef]
41. Sun, S.Y.; Salim, T.; Mathews, N.; Duchamp, M.; Boothroyd, C.; Xing, G.C.; Sum, T.C.; Lam, Y.M. The origin of high efficiency in low-temperature solution-processable bilayer organometal halide hybrid solar cells. *Energy Environ. Sci.* **2014**, *7*, 399–407. [CrossRef]
42. Wu, M.C.; Chan, S.H.; Jao, M.H.; Su, W.F. Enhanced short-circuit current density of perovskite solar cells using Zn-doped TiO_2 as electron transport layer. *Sol. Energy Mater. Sol. Cells* **2016**, *157*, 447–453. [CrossRef]
43. Wojciechowski, K.; Fang, S.D.; Abate, A.; Sadoughi, G.; Sadhanala, A.; Kopidakis, N.; Rumbles, G.; Li, C.Z.; Friend, R.H.; Jen, A.K.Y.; et al. Heterojunction Modification for Highly Efficient Organic-Inorganic Perovskite Solar Cells. *ACS Nano* **2014**, *8*, 12701–12709. [CrossRef]
44. Heo, J.H.; Han, H.J.; Kim, D.; Ahn, T.K.; Im, S.H. Hysteresis-less inverted $CH_3NH_3PbI_3$ planar perovskite hybrid solar cells with 18.1% power conversion efficiency. *Energy Environ. Sci.* **2015**, *8*, 1602–1608. [CrossRef]
45. Murugadoss, G.; Tanaka, S.; Mizuta, G.; Kanaya, S.; Nishino, H.; Umeyama, T.; Imahori, H.; Ito, S. Light stability tests of methylammonium and formamidinium Pb-halide perovskite for solar cell applications. *Jpn. J. Appl. Phys.* **2015**, *54*, 08KF08. [CrossRef]
46. Zhou, H.; Chen, Q.; Li, G.; Luo, S.; Song, T.-B.; Duan, H.-S.; Hong, Z.; You, J.; Liu, Y.; Yang, Y. Interface engineering of highly efficient perovskite solar cells. *Science* **2014**, *345*, 542–546. [CrossRef] [PubMed]
47. Sidhik, S.; Cerdan Pasarán, A.; Esparza, D.; López Luke, T.; Carriles, R.; De la Rosa, E. Improving the optoelectronic properties of mesoporous TiO_2 by cobalt doping for high-performance hysteresis-free perovskite solar cells. *ACS Appl. Mater. Interfaces* **2018**, *10*, 3571–3580. [CrossRef] [PubMed]
48. Giordano, F.; Abate, A.; Correa Baena, J.P.; Saliba, M.; Matsui, T.; Im, S.H.; Zakeeruddin, S.M.; Nazeeruddin, M.K.; Hagfeldt, A.; Graetzel, M. Enhanced electronic properties in mesoporous TiO_2 via lithium doping for high-efficiency perovskite solar cells. *Nat. Commun.* **2016**, *7*, 10379. [CrossRef] [PubMed]
49. Ranjitha, A.; Thambidurai, M.; Shini, F.; Muthukumarasamy, N.; Velauthapillai, D. Effect of doped TiO_2 film as electron transport layer for inverted organic solar cell. *Mater. Sci. Energy Technol.* **2019**, *2*, 385–388. [CrossRef]
50. Su, T.-S.; Wei, T.-C. Co-Electrodeposition of Sn-Doped TiO_2 Electron-Transporting Layer for Perovskite Solar Cells. *Phys. Status Solidi A* **2020**, *217*, 1900491. [CrossRef]
51. Wu, T.; Zhen, C.; Zhu, H.; Wu, J.; Jia, C.; Wang, L.; Liu, G.; Park, N.-G.; Cheng, H.-M. Gradient Sn-Doped Heteroepitaxial Film of Faceted Rutile TiO_2 as an Electron Selective Layer for Efficient Perovskite Solar Cells. *ACS Appl. Mater. Interfaces* **2019**, *11*, 19638–19646. [CrossRef] [PubMed]
52. Gu, X.; Wang, Y.; Zhang, T.; Liu, D.; Zhang, R.; Zhang, P.; Wu, J.; Chen, Z.D.; Li, S. Enhanced electronic transport in Fe^{3+}-doped TiO_2 for high efficiency perovskite solar cells. *J. Mater. Chem. C* **2017**, *5*, 10754–10760. [CrossRef]
53. Xu, Z.; Yin, X.; Guo, Y.; Pu, Y.; He, M. Ru-Doping in TiO_2 electron transport layers of planar heterojunction perovskite solar cells for enhanced performance. *J. Mater. Chem. C* **2018**, *6*, 4746–4752. [CrossRef]
54. Wang, S.; Liu, B.; Zhu, Y.; Ma, Z.; Liu, B.; Miao, X.; Ma, R.; Wang, C. Enhanced performance of TiO_2-based perovskite solar cells with Ru-doped TiO_2 electron transport layer. *Sol. Energy* **2018**, *169*, 335–342. [CrossRef]
55. Chen, B.-X.; Rao, H.-S.; Li, W.-G.; Xu, Y.-F.; Chen, H.-Y.; Kuang, D.-B.; Su, C.-Y. Achieving high-performance planar perovskite solar cell with Nb-doped TiO_2 compact layer by enhanced electron injection and efficient charge extraction. *J. Mater. Chem. A* **2016**, *4*, 5647–5653. [CrossRef]
56. Wu, M.-C.; Chan, S.-H.; Lee, K.-M.; Chen, S.-H.; Jao, M.-H.; Chen, Y.-F.; Su, W.-F. Enhancing the efficiency of perovskite solar cells using mesoscopic zinc-doped TiO_2 as the electron extraction layer through band alignment. *J. Mater. Chem. A* **2018**, *6*, 16920–16931. [CrossRef]
57. Lv, M.; Lv, W.; Fang, X.; Sun, P.; Lin, B.; Zhang, S.; Xu, X.; Ding, J.; Yuan, N. Performance enhancement of perovskite solar cells with a modified TiO_2 electron transport layer using Zn-based additives. *RSC Adv.* **2016**, *6*, 35044–35050. [CrossRef]
58. Ranjan, R.; Prakash, A.; Singh, A.; Singh, A.; Garg, A.; Gupta, R.K. Effect of tantalum doping in a TiO_2 compact layer on the performance of planar spiro-OMeTAD free perovskite solar cells. *J. Mater. Chem. A* **2018**, *6*, 1037–1047. [CrossRef]
59. Wang, J.; Qin, M.; Tao, H.; Ke, W.; Chen, Z.; Wan, J.; Qin, P.; Xiong, L.; Lei, H.; Yu, H.; et al. Performance enhancement of perovskite solar cells with Mg-doped TiO_2 compact film as the hole-blocking layer. *Appl. Phys. Lett.* **2015**, *106*, 121104. [CrossRef]
60. Zhang, H.; Shi, J.; Xu, X.; Zhu, L.; Luo, Y.; Li, D.; Meng, Q. Mg-doped TiO_2 boosts the efficiency of planar perovskite solar cells to exceed 19%. *J. Mater. Chem. A* **2016**, *4*, 15383–15389. [CrossRef]
61. Acchutharaman, K.R.; Santhosh, N.; Senthil Pandian, M.; Ramasamy, P. Improved optoelectronic properties of rutile TiO_2 nanorods through strontium doping for the economical and efficient perovskite solar cells. *Mater. Res. Bull.* **2023**, *160*, 112141. [CrossRef]

62. Wu, M.-C.; Liao, Y.-H.; Chan, S.-H.; Lu, C.-F.; Su, W.-F. Enhancing organolead halide perovskite solar cells performance through interfacial engineering using Ag-doped TiO_2 hole blocking layer. *Sol. RRL* **2018**, *2*, 1800072. [CrossRef]
63. Ke, W.; Fang, G.; Wang, J.; Qin, P.; Tao, H.; Lei, H.; Liu, Q.; Dai, X.; Zhao, X. Perovskite solar cell with an efficient TiO_2 compact film. *ACS Appl. Mater. Interfaces* **2014**, *6*, 15959–15965. [CrossRef] [PubMed]
64. Liang, J.; Chen, Z.; Yang, G.; Wang, H.; Ye, F.; Tao, C.; Fang, G. Achieving High Open-Circuit Voltage on Planar Perovskite Solar Cells via Chlorine-Doped Tin Oxide Electron Transport Layers. *ACS Appl. Mater. Interfaces* **2019**, *11*, 23152–23159. [CrossRef] [PubMed]
65. Arman, S.Y.; Omidvar, H.; Tabaian, S.H.; Sajjadnejad, M.; Fouladvand, S.; Afshar, S. Evaluation of nanostructured S-doped TiO_2 thin films and their photoelectrochemical application as photoanode for corrosion protection of 304 stainless steel. *Surf. Coat. Technol.* **2014**, *251*, 162–169. [CrossRef]
66. Abd Mutalib, M.; Ahmad Ludin, N.; Su'ait, M.S.; Davies, M.; Sepeai, S.; Mat Teridi, M.A.; Mohamad Noh, M.F.; Ibrahim, M.A. Performance-Enhancing Sulfur-Doped TiO_2 Photoanodes for Perovskite Solar Cells. *Appl. Sci.* **2022**, *12*, 429. [CrossRef]
67. Chen, S.-H.; Chan, S.-H.; Lin, Y.-T.; Wu, M.-C. Enhanced power conversion efficiency of perovskite solar cells based on mesoscopic Ag-doped TiO_2 electron transport layer. *Appl. Surface Sci.* **2019**, *469*, 18–26. [CrossRef]
68. Wang, Z.; Zhang, Z.; Xie, L.; Wang, S.; Yang, C.; Fang, C.; Hao, F. Recent Advances and Perspectives of Photostability for Halide Perovskite Solar Cells. *Adv. Opt. Mater.* **2022**, *10*, 2101822. [CrossRef]
69. Zaky, A.A.; Christopoulos, E.; Gkini, K.; Arfanis, M.K.; Sygellou, L.; Kaltzoglou, A.; Stergiou, A.; Tagmatarchis, N.; Balis, N.; Falaras, P. Enhancing efficiency and decreasing photocatalytic degradation of perovskite solar cells using a hydrophobic copper-modified titania electron transport layer. *Appl. Catal. B Environ.* **2021**, *284*, 119714. [CrossRef]
70. Liu, Z.; Wu, S.; Yang, X.; Zhou, Y.; Jin, J.; Sun, J.; Zhao, L.; Wang, S. The dual interfacial modification of 2D g-C_3N_4 for high-efficiency and stable planar perovskite solar cells. *Nanoscale Adv.* **2020**, *2*, 5396–5402. [CrossRef]
71. Gkini, K.; Martinaiou, I.; Botzakaki, M.; Tsipas, P.; Theofylaktos, L.; Dimoulas, A.; Katsaros, F.; Stergiopoulos, T.; Krontiras, C.; Georga, S.; et al. Energy band tuning induced by g-C_3N_4 interface engineering for efficient and stable perovskite solar cells. *Mater. Today Commun.* **2022**, *32*, 103899. [CrossRef]
72. Haque, M.A.; Sheikh, A.D.; Guan, X.; Wu, T. Metal Oxides as Efficient Charge Transporters in Perovskite Solar Cells. *Adv. Ener. Mat.* **2017**, *7*, 1602803. [CrossRef]
73. Sanehira, E.M.; Tremolet de Villers, B.J.; Schulz, P.; Reese, M.O.; Ferrere, S.; Zhu, K.; Lin, L.Y.; Berry, J.J.; Luther, J.M. Influence of Electrode Interfaces on the Stability of Perovskite Solar Cells: Reduced Degradation Using MoOx/Al for Hole Collection. *ACS Energy Lett.* **2016**, *1*, 38–45. [CrossRef]
74. Wang, Y.D.; Wang, Y.; Shao, J.Y.; Lan, Y.; Lan, Z.R.; Zhong, Y.W.; Song, Y. Defect Passivation by a D–A–D Type Hole-Transporting Interfacial Layer for Efficient and Stable Perovskite Solar Cells. *ACS Energy Lett.* **2021**, *6*, 2030–2037. [CrossRef]
75. Wang, C.; Gao, P. Radicalize the Performance of Perovskite Solar Cells with Radical Compounds. *Chem. Res. Chin. Univ.* **2023**, *39*, 176–186. [CrossRef]
76. Jiang, Q.; Ni, Z.; Xu, G.; Lin, Y.; Rudd, P.N.; Xue, R.; Li, Y.; Li, Y.; Gao, Y.; Huang, J. Interfacial Molecular Doping of Metal Halide Perovskite for Highly Efficient Solar Cells. *Adv. Mater.* **2020**, *32*, 2001581. [CrossRef] [PubMed]
77. Niu, Y.; Peng, Y.; Zhang, X.; Ren, Y.; Ghadari, R.; Zhu, J.; Tulloch, G.; Zhang, H.; Falaras, P.; Hu, L. Resonant molecular treatment for efficient and stable perovskite solar cells. *ACS Energy Lett.* **2022**, *7*, 3104–3111. [CrossRef]
78. Niazi, Z.; Hagfeldt, A.; Goharshadi, E.K. Recent progress on the use of graphene-based nanomaterials in perovskite solar cells. *J. Mater. Chem. A* **2023**, *11*, 6659–6687. [CrossRef]
79. Cho, T.; Grancini, G.; Lee, Y.; Konios, D.; Paek, S.; Kymakis, E.; Nazeeruddin, M.K. Beneficial Role of Reduced Graphene Oxide for Electron Extraction in Highly Efficient Perovskite Solar Cells. *ChemSusChem* **2016**, *9*, 3040–3044. [CrossRef]
80. Agresti, A.; Pescetelli, S.; Cinà, L.; Konios, D.; Kakavelakis, G.; Kymakis, E.; Di Carlo, A. Efficiency and Stability Enhancement in Perovskite Solar Cells by Inserting Lithium-Neutralized Graphene Oxide as Electron Transporting Layer. *Adv. Funct. Mater.* **2016**, *6*, 2686–2694. [CrossRef]
81. Yang, Q.-D.; Li, J.; Cheng, Y.; Li, H.-W.; Guan, Z.; Yu, B.; Tsang, S.-W. Graphene oxide as an efficient hole-transporting material for high-performance perovskite solar cells with enhanced stability. *J. Mater. Chem. A* **2017**, *5*, 9852–9858. [CrossRef]
82. Nouri, E.; Wang, Y.-L.; Chen, Q.; Xu, J.-J.; Paterakis, G.; Dracopoulos, V.; Xu, Z.-X.; Tasis, D.; Mohammadi, M.R.; Lianos, P. Introduction of Graphene Oxide as Buffer Layer in Perovskite Solar Cells and the Promotion of Soluble n-Butyl-substituted Copper Phthalocyanine as Efficient Hole Transporting Material. *Electrochim. Acta* **2017**, *233*, 36–43. [CrossRef]
83. Palma, A.L.; Cinà, L.; Pescetelli, S.; Agresti, A.; Raggio, M.; Paolesse, R.; Bonaccorso, F.; Di Carlo, A. Reduced graphene oxide as efficient and stable hole transporting material in mesoscopic perovskite solar cells. *Nano Energy* **2016**, *22*, 349–360. [CrossRef]
84. Balis, N.; Zaky, A.A.; Athanasekou, C.; Silva, A.M.T.; Sakellis, E.; Vasilopoulou, M.; Stergiopoulos, T.; Kontos, A.G.; Falaras, P. Investigating the Role of Reduced Graphene Oxide as a Universal Additive in Planar Perovskite Solar Cells. *J. Photochem. Photobiol. A Chem.* **2020**, *386*, 112141. [CrossRef]
85. Lin, X.; Su, H.; He, S.; Song, Y.; Wang, Y.; Qin, Z.; Wu, Y.; Yang, X.; Han, Q.; Fang, J.; et al. In situ growth of graphene on both sides of a Cu–Ni alloy electrode for perovskite solar cells with improved stability. *Nat. Energy* **2022**, *7*, 520–527. [CrossRef]
86. Wang, Y.; Wu, T.; Barbaud, J.; Kong, W.; Cui, D.; Chen, H.; Yang, X.; Han, L. Stabilizing heterostructures of soft perovskite semiconductors. *Science* **2019**, *365*, 687–691. [CrossRef]

87. Pang, S.; Zhang, C.; Zhang, H.; Dong, H.; Chen, D.; Zhu, W.; Xi, H.; Chang, J.; Lin, Z.; Zhang, J.; et al. Boosting performance of perovskite solar cells with Graphene quantum dots decorated SnO_2 electron transport layers. *Appl. Surf. Sci.* **2020**, *507*, 145099. [CrossRef]
88. Zhou, C.; Lin, H.; Tian, Y.; Yuan, Z.; Clark, R.; Chen, B.; van de Burgt, L.J.; Wang, J.C.; Zhou, Y.; Hanson, K.; et al. Luminescent Zero-Dimensional Organic Metal Halide Hybrids with near-Unity Quantum Efficiency. *Chem. Sci.* **2018**, *9*, 586–593. [CrossRef]
89. Fan, J.; Ma, Y.; Zhang, C.; Liu, C.; Li, W.; Schropp, R.E.I.; Mai, Y. Thermodynamically Self-Healing 1D–3D Hybrid Perovskite Solar Cells. *Adv. Energy Mater.* **2018**, *8*, 1703421. [CrossRef]
90. Ma, C.; Shen, D.; Huang, B.; Li, X.; Chen, W.-C.; Lo, M.-F.; Wang, P.; Hon-Wah Lam, M.; Lu, Y.; Ma, B.; et al. High Performance Low-Dimensional Perovskite Solar Cells Based on a One Dimensional Lead Iodide Perovskite. *J. Mater. Chem. A* **2019**, *7*, 8811–8817. [CrossRef]
91. Liu, Y.; Yuan, S.; Zheng, H.; Wu, M.; Zhang, S.; Lan, J.; Li, W.; Fan, J. Structurally Dimensional Engineering in Perovskite Photovoltaics. *Adv. Energy Mater.* **2023**, *356*, 2300188. [CrossRef]
92. Elsenety, M.M.; Kaltzoglou, A.; Antoniadou, M.; Koutselas, I.; Kontos, A.G.; Falaras, P. Synthesis, Characterization and Use of Highly Stable Trimethyl Sulfonium Tin(IV) Halide Defect Perovskites in Dye Sensitized Solar Cells. *Polyhedron* **2018**, *150*, 83–91. [CrossRef]
93. Elsenety, M.M.; Antoniadou, M.; Kaltzoglou, A.; Kontos, A.G.; Philippopoulos, A.I.; Mitsopoulou, C.A.; Falaras, P. Synthesis, Characterization of $((CH_3)_3S)_2SnI_{6\text{-}n}Cl_n$ and $((CH_3)_3S)_2SnI_{6\text{-}n}Br_n$ (n = 1, 2) Perovskites and Use in Dye-Sensitized Solar Cells. *Mater. Chem. Phys.* **2020**, *239*, 122310. [CrossRef]
94. Kaltzoglou, A.; Stoumpos, C.C.; Kontos, A.G.; Manolis, G.K.; Papadopoulos, K.; Papadokostaki, K.G.; Psycharis, V.; Tang, C.C.; Jung, Y.K.; Walsh, A.; et al. Trimethylsulfonium Lead Triiodide: An Air-Stable Hybrid Halide Perovskite. *Inorg. Chem.* **2017**, *56*, 6302–6309. [CrossRef] [PubMed]
95. Min, H.; Kim, G.; Paik, M.J.; Lee, S.; Yang, W.S.; Jung, M.; Seok, S.I. Stabilization of Precursor Solution and Perovskite Layer by Addition of Sulfur. *Adv. Energy Mater.* **2019**, *9*, 1803476. [CrossRef]
96. Kaltzoglou, A.; Elsenety, M.M.; Koutselas, I.; Kontos, A.G.; Papadopoulos, K.; Psycharis, V.; Raptopoulou, C.P.; Perganti, D.; Stergiopoulos, T.; Falaras, P. Synthesis, Characterization and Optoelectronic Properties of Chemically Stable $(CH_3)_3SPbI_{3-x}Br_x$ and $(CH_3)_3SPbI_{3-x}Cl_x$ (X = 0, 1, 2, 3) Perovskites. *Polyhedron* **2018**, *140*, 67–73. [CrossRef]
97. Kaltzoglou, A.; Manolis, G.K.; Elsenety, M.M.; Koutselas, I.; Psycharis, V.; Kontos, A.G.; Falaras, P. Synthesis and Characterization of Lead-Free $(CH_3)_3SSnI_3$ 1-D Perovskite. *J. Electron. Mater.* **2019**, *48*, 7533–7538. [CrossRef]
98. Elsenety, M.; Antoniadou, M.; Balis, N.; Kaltzoglou, A.; Sygellou, L.; Stergiou, A.; Tagmatarchis, N.; Falaras, P. Stability Improvement and Performance Reproducibility Enhancement of Perovskite Solar Cells Following (FA/MA/Cs) $PbI_{3-x}Br_x/(CH_3)_3SPbI_3$ Dimensionality Engineering. *ACS Appl. Energy Mater.* **2020**, *3*, 2465–2477. [CrossRef]
99. Parashar, M.; Singh, R.; Yoo, K.; Lee, J.-J. Formation of 1-D/3-D Fused Perovskite for Efficient and Moisture Stable Solar Cells. *ACS Appl. Energy Mater.* **2021**, *4*, 2751–2760. [CrossRef]
100. Lin, Y.; Shen, L.; Dai, J.; Deng, Y.; Wu, Y.; Bai, Y.; Zheng, X.; Wang, J.; Fang, Y.; Wei, H.; et al. π-Conjugated Lewis Base: Efficient Trap-Passivation and Charge-Extraction for Hybrid Perovskite Solar Cells. *Adv. Mater.* **2017**, *29*, 1604545. [CrossRef]
101. Wu, Z.; Raga, S.R.; Juarez-Perez, E.J.; Yao, X.; Jiang, Y.; Ono, L.K.; Ning, Z.; Tian, H.; Qi, Y. Improved Efficiency and Stability of Perovskite Solar Cells Induced by C=O Functionalized Hydrophobic Ammonium-Based Additives. *Adv. Mater.* **2018**, *3*, 1703670. [CrossRef] [PubMed]
102. Kim, W.; Bae Park, J.; Kim, H.; Kim, K.; Park, J.; Cho, S.; Lee, H.; Pak, Y.; Jung, G.Y. Enhanced long-term stability of perovskite solar cells by passivating grain boundary with polydimethylsiloxane (PDMS). *J. Mater. Chem. A* **2019**, *7*, 20832–20839. [CrossRef]
103. Li, X.; Chen, C.-C.; Cai, M.; Hua, X.; Xie, F.; Liu, X.; Hua, J.; Long, Y.-T.; Tian, H.; Han, L. Efficient Passivation of Hybrid Perovskite Solar Cells Using Organic Dyes with -COOH Functional Group. *Adv. Energy Mater.* **2018**, *8*, 1800715. [CrossRef]
104. Wu, T.; Wang, Y.; Li, X.; Wu, Y.; Meng, X.; Cui, D.; Yang, X.; Han, L. Efficient Defect Passivation for Perovskite Solar Cells by Controlling the Electron Density Distribution of Donor-π-Acceptor Molecules. *Adv. Energy Mater.* **2019**, *9*, 1803766. [CrossRef]
105. Fu, S.; Li, X.; Wan, L.; Wu, Y.; Zhang, W.; Wang, Y.; Bao, Q.; Fang, J. Efficient Passivation with Lead Pyridine-2-Carboxylic for High-Performance and Stable Perovskite Solar Cells. *Adv. Energy Mater.* **2019**, *9*, 1901852. [CrossRef]
106. Cao, J.; Li, C.; Lv, X.; Feng, X.; Meng, R.; Wu, Y.; Tang, Y. Efficient Grain Boundary Suture by Low-Cost Tetra-ammonium Zinc Phthalocyanine for Stable Perovskite Solar Cells with Expanded Photoresponse. *J. Am. Chem. Soc.* **2018**, *140*, 11577. [CrossRef] [PubMed]
107. Elsenety, M.; Stergiou, A.; Sygellou, L.; Tagmatarchis, N.; Balis, N.; Falaras, P. Boosting Perovskite Nanomorphology and Charge Transport Properties via a Functional D-π-A Organic Layer at the Absorber/Hole Transporter Interface. *Nanoscale* **2020**, *12*, 15137–15149. [CrossRef]
108. Zhang, T.; Yang, X.; Zhang, L.; Deng, Z.; Yang, K.; Cui, H.; Hou, Q.; Ji, W. A D–π–A Organic Dye as a Passivator to Effectively Regulate the Performance of Perovskite Solar Cells. *Energy Technol.* **2022**, *10*, 220026. [CrossRef]
109. Koh, T.M.; Shanmugam, V.; Guo, X.; Lim, S.S.; Filonik, O.; Herzig, E.M.; Muller-Buschbaum, P.; Swamy, V.; Chien, S.T.; Mhaisalkar, S.G.; et al. Enhancing moisture tolerance in efficient hybrid 3D/2D perovskite photovoltaics. *J. Mater. Chem. A* **2018**, *6*, 2122–2128. [CrossRef]

110. Saidaminov, M.I.; Kim, J.; Jain, A.; Quintero-Bermudez, R.; Tan, H.; Long, G.; Tan, F.; Johnston, A.; Zhao, Y.; Voznyy, O.; et al. Suppression of atomic vacancies via incorporation of isovalent small ions to increase the stability of halide perovskite solar cells in ambient air. *Nat. Energy* **2018**, *3*, 648–654. [CrossRef]
111. Zhao, W.; Shi, J.; Tian, C.; Wu, J.; Li, H.; Li, Y.; Yu, B.; Luo, Y.; Wu, H.; Xie, Z.; et al. CdS Induced Passivation toward High Efficiency and Stable Planar Perovskite Solar Cells. *ACS Appl. Mater. Interfaces* **2021**, *13*, 9771–9780. [CrossRef]
112. Wu, Z.; Jiang, M.; Liu, Z.; Jamshaid, A.; Ono, L.K.; Qi, Y. Highly Efficient Perovskite Solar Cells Enabled by Multiple Ligand Passivation. *Adv. Energy Mater.* **2020**, *10*, 1903696. [CrossRef]
113. Zhang, K.; Wang, Z.; Wang, G.; Wang, J.; Li, Y.; Qian, W.; Zheng, S.; Xiao, S.; Yang, S. A prenucleation strategy for ambient fabrication of perovskite solar cells with high device performance uniformity. *Nat. Commun.* **2020**, *11*, 1006. [CrossRef] [PubMed]
114. He, D.; Xu, X.; Liang, Z.; Niu, Y.; Sun, Y.; Tulloch, G.; Falaras, P.; Hu, L. Defect passivation and humidity protection for perovskite solar cells enabled by 1-dodecanethiol. *J. Mater. Chem. C* **2021**, *9*, 9584–9591. [CrossRef]
115. Kara, D.A.; Cirak, D.; Gultekin, B. Decreased surface defects and non-radiative recombination via the passivation of the halide perovskite film by 2-thiophenecarboxylic acid in triple-cation perovskite solar cells. *Phys. Chem. Chem. Phys.* **2022**, *24*, 10384. [CrossRef]
116. Kim, J.W.; Park, H.; Lee, G.; Jeong, Y.R.; Hong, S.Y.; Keum, K.; Yoon, J.; Kim, M.S.; Ha, J.S. Paper-Like, Thin, Foldable, and Self-Healable Electronics Based on PVA/CNC Nanocomposite Film. *Adv. Funct. Mater.* **2019**, *29*, 1905968. [CrossRef]
117. Jiang, Y.; Qiu, L.; Juarez-Perez, E.J.; Ono, L.K.; Hu, Z.; Liu, Z.; Wu, Z.; Meng, L.; Wang, Q.; Qi, Y. Reduction of lead leakage from damaged lead halide perovskite solar modules using self-healing polymer-based encapsulation. *Nat. Energy* **2019**, *4*, 585–593. [CrossRef]
118. Gong, Z.; He, B.; Zhu, J.; Yao, X.; Wang, S.; Chen, H.Y.; Duan, Y.Y.; Tang, Q. Tri-Brominated Perovskite Film Management and Multiple-Ionic Defect Passivation for Highly Efficient and Stable Solar Cells. *Sol. RRL* **2021**, *5*, 2000819. [CrossRef]
119. Wang, M.; Sun, H.; Cao, F.; Tian, W.; Li, L. Moisture-Triggered Self-Healing Flexible Perovskite Photodetectors with Excellent Mechanical Stability. *Adv. Mater.* **2021**, *33*, 2100625. [CrossRef]
120. Zhu, J.; Tang, M.; He, B.; Shen, K.; Zhang, W.; Sun, X.; Sun, M.; Chen, H.; Duan, Y.; Tang, Q. Ultraviolet filtration and defect passivation for efficient and photostable $CsPbBr_3$ perovskite solar cells by interface engineering with ultraviolet absorber. *Chem. Eng. J.* **2021**, *404*, 126548. [CrossRef]
121. Xu, Q.; Zhang, H.; Nie, J.; Shao, W.; Wang, X.; Zhang, B.; Ouyang, X. Effect of methylammonium lead tribromide perovskite based-photoconductor under gamma photons radiation. *Radiat. Phys. Chem.* **2021**, *181*, 109337. [CrossRef]
122. Niu, Y.; He, D.; Zhang, Z.; Zhu, J.; Tulloch, G.; Falaras, P.; Hua, L. Improved crystallinity and self-healing effects in perovskite solar cells via functional incorporation of polyvinylpyrrolidone. *J. Energy Chem.* **2022**, *68*, 12–18. [CrossRef]
123. Jing, Y.; Wang, C.; Chen, Y.; Liu, L.; Yin, L.; Cui, F.; Zhang, N.; Wen, S.; Zhu, G. Crystallinity Regulation and Defects Passivation for Efficient and Stable Perovskite Solar Cells Using Fully Conjugated Porous Aromatic Frameworks. *Angew. Chem. Int. Ed.* **2023**, *62*, e202301234. [CrossRef]
124. Yu, Y.-Y.; Tseng, C.; Chien, W.-C.; Hsu, H.-L.; Chen, C.-P. Photovoltaic Performance Enhancement of Perovskite Solar Cells Using Polyimide and Polyamic Acid as Additives. *J. Phys. Chem. C* **2019**, *123*, 23826–23833. [CrossRef]
125. Chowdhury, T.A.; bin Zafar, M.A.; Islam, M.S.-U.; Shahinuzzaman, M.M.; Islam, M.A.; Khandaker, M.U. Stability of perovskite solar cells: Issues and prospects. *RSC Adv.* **2023**, *13*, 1787. [CrossRef] [PubMed]
126. Wang, F.; Bai, S.; Tress, W.F.; Hagfeldt, A.; Gao, F. Defects engineering for high-performance perovskite solar cells. *npj Flex Electron.* **2018**, *2*, 22. [CrossRef]
127. Sherkar, T.S.; Momblona, C.; Gil-Escrig, L.; Ávila, J.; Sessolo, M.; Bolink, H.J.; Koster, L.J.A. Recombination in Perovskite Solar Cells: Significance of Grain Boundaries, Interface Traps, and Defect Ions. *ACS Energy Lett* **2017**, *2*, 1214. [CrossRef]
128. Yin, W.J.; Shi, T.; Yan, Y. Unusual defect physics in $CH_3NH_3PbI_3$ perovskite solar cell absorber. *Appl. Phys. Lett.* **2014**, *104*, 063903. [CrossRef]
129. Gong, X.; Guan, L.; Pan, H.; Sun, Q.; Zhao, X.; Li, H.; Pan, H.; Shen, Y.; Shao, Y.; Sun, L.; et al. Highly Efficient Perovskite Solar Cells via Nickel Passivation. *Adv. Funct. Mater.* **2018**, *28*, 1804286. [CrossRef]
130. Feng, X.; Chen, R.; Nan, Z.-A.; Lv, X.; Meng, R.; Cao, J.; Tang, Y. Perfection of Perovskite Grain Boundary Passivation by Eu-Porphyrin Complex for Overall-Stable Perovskite Solar Cells. *Adv. Sci.* **2019**, *6*, 1802040. [CrossRef]
131. Tao, Q.; Xu, P.; Li, M.; Lu, W. Machine learning for perovskite materials design and discovery. *NPJ Comput. Mater.* **2021**, *7*, 23. [CrossRef]
132. Yılmaz, B.; Yıldırım, R. Critical review of machine learning applications in perovskite solar research. *Nano Energy* **2021**, *80*, 105546. [CrossRef]
133. Raccuglia, P.; Elbert, K.C.; Adler, P.D.F.; Falk, C.; Wenny, M.B.; Mollo, A.; Zeller, M.; Friedler, S.A.; Schrier, J.; Norquist, A.J. Machine-learning-assisted materials discovery using failed experiments. *Nature* **2016**, *533*, 73. [CrossRef]
134. Balachandran, P.V.; Kowalski, B.; Sehirlioglu, A.; Lookman, T. Experimental search for high-temperature ferroelectric perovskites guided by two-step machine learning. *Nat. Commun.* **2018**, *9*, 1668. [CrossRef]
135. She, C.; Huang, Q.; Chen, C.; Jiang, Y.; Fan, Z.; Gao, J. Machine learning-guided search for high-efficiency perovskite solar cells with doped electron transport layers. *J. Mater. Chem. A* **2021**, *9*, 25168–25177. [CrossRef]
136. Elsenety, M.M.; Christopoulos, E.; Falaras, P. Passivation Engineering Using Ultra-Hydrophobic Organic D-π-A dye with Machine Learning insights for Efficient and Stable Perovskite Solar Cells. *Solar RRL* **2023**, *7*, 2201016. [CrossRef]

137. Zhang, L.; Hu, W. Molecular design for perovskite solar cells. *Int. J. Energy Res.* **2022**, *46*, 14740–14765. [CrossRef]
138. Zhang, L.; Wenguang Hu, W.; Li, S. Optimizing Photoelectrochemical Photovoltage and Stability of Molecular Interlayer-Modified Halide Perovskite in Water: Insights from Interpretable Machine Learning and Symbolic Regression. *ACS Appl. Energy Mater.* **2023**, *6*, 5177–5187. [CrossRef]